LA-UR- 98-1677

Approved for public release; distribution is unlimited.

Title: THREE-BODY COLLISION CONTRIBUTIONS TO RECOMBINATION AND COLLISION-INDUCED DISSOCIATION. II. KINETICS

Author(s): Russell T Pack
Robert B. Walker
Brian Kendrick

Submitted to: Journal of Chemical Physics

Los Alamos
NATIONAL LABORATORY

DISCLAIMER

DISCLAIMER

Portions of this document may be illegible in electronic image products. Images are produced from the best available original document.

LA-UR-98-0000

THREE-BODY COLLISION CONTRIBUTIONS TO RECOMBINATION AND COLLISION-INDUCED DISSOCIATION. II. KINETICS

Russell T Pack, Robert B. Walker, and Brian K. Kendrick

Theoretical Division (T-12, MS B268), Los Alamos National Laboratory, Los Alamos, New Mexico 87545

(April 10, 1998)

Abstract

Detailed rate constants for the reaction $Ne + Ne + H \rightleftharpoons Ne_2 + H$ are generated, and the master equations governing collision-induced dissociation (CID) and recombination are accurately solved numerically. The temperature and pressure dependence are explored. At all pressures, three-body (3B) collisions dominate. The sequential two-body energy-transfer (ET) mechanism gives a rate that is more than a factor of two too small at low pressures and orders of magnitude too small at high pressures. Simpler models are explored; to describe the kinetics they must include direct 3B rates connecting the continuum to the bound states and to the quasibound states. The relevance of the present reaction to more general CID/recombination reactions is discussed. For atomic fragments, the 3B mechanism usually dominates. For diatomic fragments, the 3B and ET mechanism are competitive, and for polyatomic fragments the ET mechanism usually dominates.

Ms number 000000JCP. PACS numbers: 34.10.+x, 82.20.Hf, 82.30.Lp, 82.30.Nr

I. INTRODUCTION

In the preceding paper,[1] herein called I, we discussed the fundamental processes of atomic and molecular recombination and collision-induced dissociation (CID). The overall chemical equation for any recombination is the forward direction of the reaction,

$$A + B + M \rightleftharpoons AB + M, \tag{1}$$

where A and B are any atoms, molecules, or radicals for which AB has bound states, and M is any species that can carry away the excess energy. The overall equation for CID is simply the reverse direction of Reaction (1). We noted in I that in most chemical kinetics literature, both textbooks and journals, recombination is assumed to proceed via two collisional mechanisms, the energy transfer (ET) and bound complex (BC) mechanisms, both of which are sequences of two-body collisions. To keep interpretation of the results clear, the discussion in I was then limited to cases where the BC mechanism cannot contribute, i.e., where species AM and BM have no bound states. Then, the competition is between direct three-body (3B) processes symbolized by Eq.(1) and the energy transfer (ET) mechanism,[1]

$$A + B \rightleftharpoons AB^*, \tag{2}$$

$$AB^* + M \rightleftharpoons AB + M. \tag{3}$$

Here species with an asterisk, such as AB^*, represent metastable intermediates.

We[1] reviewed the literature and found that in the first two-thirds of this century, most papers and texts allowed for true 3B collisions but were unable to accurately estimate their rates. However, the more recent literature is confusing. Due at least in part to Roberts, Bernstein, and Curtiss' (RBC)[2] "orbiting resonance theory" (ORT) of the ET mechanism of atomic recombination, their identification of the AB^* as quasibound (QB) states of the diatomic AB trapped behind an angular momentum barrier, and their arguments that direct 3B contributions are small, many of the more recent books and papers either do not mention possible contributions of 3B collisions or are so indefinite that many physical chemists do

not even consider the possibility of 3B collisions in interpreting data. This state of affairs is strange considering that important contributions due to 3B collisions are implied by the ortho-para ratios of H_2 formed by recombination of H atoms, the pressure dependence of the rates of recombination of atoms and diatomic radicals, the success of classical calculations of atomic recombination and CID (which can only happen classically via 3B collisions), and the great importance of 3B collisional rates in the many master equation studies of the CID and recombination of H atoms that have been reported.[1]

In order to clarify the relative roles of the ET and 3B mechanisms, we,[1] in paper I, performed calculations on the recombination of Ne atoms and the CID of Ne_2 dimers in the presence of H atoms,

$$Ne + Ne + H \rightleftharpoons Ne_2 + H, \tag{4}$$

using the Vibrational and Rotational Infinite Order Sudden (VRIOS) approximation which treats bound, quasibound (metastable), and continuum states on the same footing and is expected to be semiquantitatively accurate for this reaction. The results clearly show that both the excited bound states and the quasibound (QB) states have large *collision* cross sections connecting them directly to the 3B continuum.

In the present work, in the next Section, we thermally average those cross sections to get rate constants that maintain detailed balance. Then, we solve the detailed master equations of the kinetics, including all the relevant states, and examine the effect of pressure, temperature, and mechanism restrictions on the effective rates of recombination and CID. Then, in Section III we discuss simple kinetics models to clarify the important reactions occurring. We also discuss the similarities and differences between this reaction and more general CID and recombination reactions. Finally, Section IV contains our conclusions.

II. MASTER EQUATIONS

In this section we use the cross sections of paper I to construct rate constants and master equations describing the kinetics of recombination and CID, solve the equations numerically for the general case and several special cases, and discuss the results.

A. Calculation of Rate Constants

Rate constants corresponding to all the cross sections of paper I were calculated using the usual formula,[3]

$$k_{fi}(T) = \bar{v}\frac{1}{(k_B T)^2}\int_0^\infty \sigma(f \leftarrow i; E)\exp(-E/(k_B T)EdE, \tag{5}$$

where k_B is Boltzmann's constant, T is the absolute temperature, E is the incident relative energy of the $M - AB$ collision, $\bar{v} = (8k_B T/\pi\mu_{M-AB})^{\frac{1}{2}}$ is the average relative velocity of the collision, and μ_{M-AB} is the $M - AB$ reduced mass. In the present calculations, with $A = B = Ne$ and $M = H$, the integrals were performed using 7-point Laguerre quadrature, and 5-point Lagrange interpolation was used to get the cross sections at energies between those at which they were calculated in paper I. We note that use of Eq. (5) implies that the distribution of relative velocities between the centers of mass of the AB pairs and the M atoms is a Boltzmann distribution which is an excellent approximation in most CID and recombination experiments.

B. Detailed Balance

Because the VRIOS approximation used to generate the cross sections in paper I does not exactly handle energy thresholds, its cross sections do not exactly satisfy the principle of microscopic reversibility,[4] and, consequently, the rate constants from Eq. (5) do not automatically exactly satisfy detailed balance.[4] Satisfying detailed balance is essential to get kinetics equations which go to the correct equilibrium. For all states i and f which are

either bound or QB states, detailed balance was easily achieved by keeping the k_{fi} from Eq.(5) only for the downward transitions ($\epsilon_f < \epsilon_i$ in Table I of paper I), where there is no threshold, and then using them and the usual[5] relationship,

$$k_{if}(T) = \frac{(2j_i+1)\exp(-\epsilon_i/k_BT)}{(2j_f+1)\exp(-\epsilon_f/k_BT)} k_{fi}(T), \tag{6}$$

to obtain rate constants, for the upward transitions from state f to state i, that exactly satisfy detailed balance. We note that inclusion of the QB states in this process is consistent with their representation in paper I by square integrable wavefunctions.

However, for transitions involving the other continuum states, both the nonresonant continuum and broad above barrier (BAB) resonances, it was convenient in paper I to only calculate cross sections *into* such states, *i.e.*, $\sigma(f \leftarrow i)$, where f represents the continuum and i represents a bound or QB state. We note that, in calculating them, one might gain some accuracy by forcing the $d\sigma/d\kappa$ of paper I to go to zero at energy thresholds. While such a procedure might change some of the smaller, unimportant rate constants, we estimate it would change the rate constants that are large enough to be important to the kinetics by less than 15% and thus not alter the conclusions of the present work. Accordingly, Eq. (5) was used to generate these k_{fi} directly. Then, to satisfy detailed balance, we note that the terms in the master equations representing the change of population in state i due to flux out into and back from state f are

$$dn_i/dt = -k_{fi}n_in_M + k_{if}n_fn_M, \tag{7}$$

where the n's are number densities. At equilibrium, detailed balance requires that

$$n_i/n_f = k_{if}/k_{fi} \equiv K_{if}. \tag{8}$$

Similarly, when state f is in equilibrium with the whole continuum (C) population of free A and B atoms, then

$$\frac{n_f}{n_An_B} = K_{fC}. \tag{9}$$

density is constant. Then, the master equations governing the kinetics take the form, for $i = 1, 2, ...11$,

$$\frac{dn_i}{dt} = -\sum_{f=1}^{11} k_{fi} n_i n_{13} + \sum_{f=1}^{11} k_{if} n_f n_{13} - k_{Ci} n_i n_{13} + k_{iC} n_{12}^2 n_{13} - k_{tout}(i) n_i + k_{tin}(i) n_{12}^2. \quad (13)$$

For $i = 12$, the Ne atom number density, the master equation is

$$\frac{dn_{12}}{dt} = 2\sum_{i=1}^{11} k_{Ci} n_i n_{13} - 2\sum_{i=1}^{11} k_{iC} n_{12}^2 n_{13} + 2\sum_{i=1}^{11} k_{tout}(i) n_i - 2\sum_{i=1}^{11} k_{tin} n_{12}^2, \quad (14)$$

and for $i = 13$, the H atom number density, it is

$$\frac{dn_{13}}{dt} = 0. \quad (15)$$

In these equations, one has

$$k_{Ci} = \sum_{f=12}^{26} k_{fi} \quad (16)$$

and

$$k_{iC} = \sum_{f=12}^{26} k_{fi} K_{iC} = k_{Ci} K_{iC}. \quad (17)$$

Also, $k_{tin}(i)$ and $k_{tout}(i)$ are the rates for quantum tunneling into and out of state i. They are zero except for the QB states $i = 9, ...11$.

The calculated rate constants for the $Ne_2 - H$ system at a temperature of 30 K are listed in Tables I and II. Because they describe elementary processes they are truly constants, independent of concentrations, that depend only on the temperature. The collisional rates are in Table I. The columns of the matrix are labeled by the initial states; the rows are labeled by the final states, so that the matrix is k_{fi}. The upper left 11×11 part of the matrix gives the constants for the rates involving all combinations of bound and quasibound states. The last row gives the rate constants for direct collision-induced dissociation of each of the bound and QB states. The last column gives the rate constants for the formation of each of the bound and QB states directly from the continuum. This last column involves three-body collisions and has the units of a termolecular reaction. The rest of the elements

in the matrix have the units of bimolecular collisions as there are two particles incident in the collision. Table II gives the rate constants for tunneling out of and into each of the three quasibound states of Ne_2. The outward tunneling rates k_{tout} are just $1/\tau_e$, where the τ_e of the quasibound states are those given in Table I of paper I. They have unimolecular units. The inward tunneling rates are simply given by

$$k_{tin}(i) = k_{tout}(i) K_{iC}. \tag{18}$$

They have bimolecular units. We remark that the ratio of inward to outward tunneling rates in this equation is the same as the ratio of inward to outward collisional rates given by Eq. (17) due to equilibrium constraints. Furthermore, from the last few terms in Eq. (13), one sees that the relative importance of 3B collisions and tunneling in populating and depopulating the QB states is controlled by the number density (pressure) of third-body (H) atoms. The number density at which the 3B and tunneling rates are equal for the i-th QB state is given by

$$n_{13}^{equal}(i) = k_{tout}(i)/k_{Ci} = k_{tin}(i)/k_{iC}. \tag{19}$$

The number densities (particles/cm^3) at which this equality occurs for each of the QB states are given as the last line of Table II. The number density at a pressure of one atmosphere at 30 K is 2.4463×10^{20}, so that one sees that, for all third-body pressures greater than 3×10^{-5} atm, the narrow (0,10) QB state is populated faster by 3B collisions than by tunneling, and that, for all third-body pressures of 1 atm or greater, all the QB states are populated faster by 3B collisions than by tunneling.

Before continuing, let us discuss an assumption made in deriving these master equations and Eq. (11) in particular. It was assumed that all the continuum $Ne - Ne$ states except the QB states always maintain equilibrium with each other and the whole free atomic Ne continuum. To rigorously prove this assumption would require detailed calculations of the $Ne - Ne$ pair distribution function as a function of distance, energy, angular momentum and time using generalizations of the theories of Flannery[7] and Lowry and Snider,[8] and such

is beyond the scope of this paper. However, we find the following arguments convincing. First, the nonresonant $Ne - Ne$ continuum states are simply part of the free atom continuum, and their distribution, which is maintained by all the $Ne - H$ and $Ne - Ne$ elastic collisions, is not of concern here. However, maintaining a population of BAB resonant states in equilibrium with the nonresonant continuum is of more concern. The BAB resonances have positive lifetimes and enhanced wavefunction amplitude in the interaction region, and their τ_e represents the time required for a $Ne - Ne$ collision at the right energy and angular momentum to build up that enhanced amplitude. As a result, if one were to use Eq. (7) of paper I, which describes the steady-state population of intermediate AB^* states under the ET mechanism assumption, and were to estimate the two terms in its denominator, one might conclude that, at high pressures of the third body ($M = H$), the populations of the narrower BAB resonances could be depleted relative to equilibrium with the free atom population. However, that would be misleading because the ET mechanism (Eq. (7) of paper I) only allows repopulation of the intermediate AB^* by two-body collisions. Actually, the BAB states have large 3B rates of populating and depopulating them which keep them in equilibrium with the rest of the atomic continuum and which increase as the third-body pressure increases, so that they never get depleted. In fact, as we show in detail in a later subsection, the broader QB states (which we *do* follow in detail) have such large 3B rates connecting them to the free atom continuum that they stay very close to in equilibrium with it. Since the narrowest of the BAB resonances has a lifetime that is more than seven times shorter than that of the broadest QB state and even larger 3B connections to the rest of the free atom continuum, the assumed equilibrium is maintained to an excellent approximation.

D. Solution of Master Equations

The set of 13 master equations just discussed was easily integrated using the DDRIV system routines for solving ordinary differential equations. It usually required less than 2 seconds of cpu time on an HP 735 workstation to follow the equations all the way to

equilibrium.

The results of such a calculation are shown in Figure 1 for a recombination case in which the initial number densities of all the bound and QB states are zero, the initial number density of Ne atoms is 2.4463×10^{16} molecules/cc (1×10^{-4} atm), that of H atoms is 2.4463×10^{20} (1 atm), and the temperature is 30 K. The details of labelling are in the figure caption. One sees that there is a wide range (a factor of about 15) in the rates at which the different states relax toward their equilibrium values, with the ground (0,0) state relaxing most slowly ($\sim$ 110 ps) and the broad QB states relaxing most rapidly ($\sim$ 8 ps). The other relaxation times are between those extremes with those of the narrow QB state and the highest-lying bound states being next most rapid.

To get a simpler figure to discuss, we plot in Figure 2, for the same calculation, the total number densities of the QB states and bound states as functions of time. We note that at this temperature (30 K) the final number density of the QB states is significant, and that is different from recombination experiments involving strongly bound diatomic molecules.

To compare these results with those of the RBC-ET theory[2] which allows only sequential two-body collisions, we simply set all the 3B collisional rates (column 12 and row 12 in Table I) to zero and rerun the calculation under otherwise the same conditions. (This is actually still slightly more general than the RBC theory because it includes both upward and downward transitions between all the bound and QB states.) The results are in Figure 3. One sees immediately that the population of bound states (solid circles) grows much more slowly than in Figure 2. Hence, it is clear that for this system under these conditions, three-body collisions actually *dominate* the recombination.

Another special case solution of the master equations is also of interest. To test the role of quantum tunneling, we now keep the 3B rates nonzero but set the tunneling rates (the first two lines of Table II) to zero and rerun the calculation under otherwise the same conditions as for Figure 1 and 2. We call this the "3B only" approximation as it is equivalent to assuming that *all* recombination occurs via 3B collisions. The results are in Figure 4, and they are very similar to Figure 2; on superposing them, one finds that the population

in the QB states rises a little more slowly than in Figure 2, but the bound state population differs by only about the width of the line on the plot. Thus, omitting tunneling has almost negligible effect on the recombination rate under these conditions. The smallness of this effect is an example of what is called a "network effect."[9,10] It is that, when many paths are allowed for some process and some minor paths are shut off, the system can adjust via the other paths and still proceed at almost the same rate. We also note that all the processes and states included in the calculation of Figure 4 have classical analogs. Hence, we expect that classical mechanics would do quite well in describing the recombination of Ne atoms in H.

E. Effective Rate Coefficients

To make quantitative comparisons of the results of solving the master equations for various cases but still keep the discussion simple and understandable, we need to consider the question of what is the effective (observable or phenomenological) "rate constant" or rate coefficient here. The fact that the master equations can easily be solved as accurately as desired does not itself give any simple interpretations.[11] And, from Figure 1, it is clear that the number densities of the different states of Ne_2 relax to their final values at many different rates.

One procedure that is often followed is to write (at least approximately) the master equations as a set of pseudo-first order equations, diagonalize the resulting rate matrix, and identify its smallest eigenvalue with the physical rate coefficient. That procedure can be done in this case, and the rate obtained is similar to the rate at which the ground (0,0) state relaxes. However, because the higher states of Ne_2 have rotational degeneracies that are much higher and energies that are only a little higher than the ground state, little of the final population ends up in the ground state, and the population as a whole relaxes somewhat faster than that of the ground state. Hence, that approach was not used for this particular system.

Suppose we let $[Ne_2]$ be the total number density of bound states. Another way to get a recombination rate coefficient is to take its rate of change $d[Ne_2]/dt$ and divide that by the atomic concentrations. However, such a rate "constant" is not at all constant with time in this case–it falls off rapidly because the excited bound states fill up and redissociation becomes rapid. Using its initial value also does not lead to useful comparisons because the initial number densities of the QB states are zero, and this gives an initial value of the rate as zero for the RBC case. The initial value for the full master equation case is 1.504×10^{-31} cc^2/sec, which is simply the sum of the first eight rows of the right hand column of Table I and is the total direct 3B rate of formation of bound states.

A better way it seems to us is to view the bound state populations as functions of time in Figures 2 through 4 as the results of experiments and analyze them simply by assuming that

$$d[Ne_2]/dt = k_r^{(3)}[Ne]^2[H] - k_d[Ne_2][H], \tag{20}$$

where k_d is a dissociation rate coefficient, and $k_r^{(3)}$ is a third-order effective recombination rate coefficient. Because $[H]$ is constant for a given "experiment," $k_r^{(3)}$ can be replaced by the equivalent effective second-order coefficient,

$$k_r^{(2)} = k_r^{(3)}[H] \tag{21}$$

which can be plotted vs. $[H]$ to look for falloff, and k_d can be similarly replaced by the effective first-order (unimolecular) rate coefficient, $\kappa_d = k_d[H]$. Furthermore, at these temperatures and pressures, a negligible fraction of the Ne atoms gets converted to QB or bound dimers, so that $[Ne]$ stays constant and equal to its equilibrium number density in these recombination "experiments." Thus,

$$[Ne]^2 = K_{eq}[Ne_2^{eq}] \tag{22}$$

where this equilibrium constant K_{eq} is 3.470×10^{20} at 30 K. Substitution into Eq.(20), with the obvious identification $\kappa_d = k_r^{(2)} K_{eq}$, produces

$$d[Ne_2]/dt = \kappa_d([Ne_2^{eq}] - [Ne_2]), \tag{23}$$

which is a simple, first-order relaxation equation whose solution is

$$[Ne_2](t) = [Ne_2^{eq}](1 - \exp(-\kappa_d t) \tag{24}$$

Solving this equation for κ_d and using the results of Figure 2 as input data, one obtains κ_d and thus k_d, $k_r^{(2)}$, and $k_r^{(3)}$ as functions of time. The resulting $k_r^{(3)}$ from both Figure 2 (exact "experiment") and the RBC-ET approximation (Figure 3) are shown in Figure 5. One sees, as expected, that the relaxation is not simply a single exponential, and these rate coefficients are not constant with time. The exact coefficient starts with the value of 1.504×10^{-31} cc^2/sec which is the direct 3B free to bound rate. Then, as the QB states begin to fill and contribute to populating the bound states, it rises. Then, as the excited bound states fill up and the process becomes limited by the rates of rovibrational relaxation into the lower bound states, the rate coefficient falls to lower than its initial value and approaches a constant value. While the RBC-ET approximation has a different initial transient behavior, its rate coefficient also approaches a constant, and these long time results can be directly compared. At 1000 picoseconds the value of the exact $k_r^{(3)}$ is 1.169×10^{-31}, while the RBC-ET approximation gives 3.537×10^{-32}, so that the RBC-ET rate coefficient is thus more than 3 times too small. The $k_r^{(3)}$ of the "3B only" approximation (not shown) looks very much like the exact result except that it lacks a maximum; it starts at the same value as the exact result but then monotonically declines to a value of 1.136×10^{-31} at 1000 psec, which is only 3% smaller than the exact result. We note, that in a real experiment, experimental noise might make it difficult to see all of the initial transient and also difficult to measure the tiny difference between the bound state concentration and its final equilibrium at very long times, so that experimental data would be taken at intermediate times, giving a larger effective rate coefficient and leaving the RBC-ET mechanism as an even poorer approximation.

F. Pressure Dependence of Rate Coefficient

The calculations described in the preceding subsections were repeated for a six order of magnitude range of number densities of the third-body gas. The resulting long time recombination rate coefficients $k_r^{(3)}$ are given in Table III and plotted in Figure 6a. One sees that the exact $k_r^{(3)}$ varies only slightly with pressure with the highest pressure result only 7% smaller than the lowest pressure result. The result of the "3B only" approximation is not shown because it is 1.136×10^{-31} independent of pressure, and the RBC-ET result varies too much to show on this plot. At the highest pressures, $k_r^{(3)}$ is flat because 3B collisions are totally dominating over any tunneling, and the exact result thus becomes equal to that of the 3B only approximation. At the lowest pressures, $k_r^{(3)}$ is flat because the tunneling is dominating over 3B collisions in populating the two broad QB states. From the table one sees that the RBC-ET approximation does better at low pressures, but it is still a factor of 2.3 times smaller than the exact result; the reason it does not approach the exact result is because there are many 3B paths in the kinetics which go directly from the free continuum into the bound states. For this system 3B collisions dominate the recombination at all pressures, and the "3B only" approximation is only 7% low at this lowest third-body pressure.

At high third-body number densities (pressures) the RBC-ET result becomes as much as three orders of magnitude too small. This is illustrated graphically by plotting the second order recombination rate coefficients (obtained from the data in Table III) versus third-body number density in Figure 6b. There one sees that the exact second order coefficient is proportional to the third-body number density at all densities. The curvature in it, caused by the variation in Figure 6a, is too small to be seen on this plot. On the other hand, the RBC-ET $k_r^{(2)}$ curves to become constant at high pressures. This clear "falloff" behavior, which is seen experimentally in the recombination of polyatomic fragments, is not seen in atomic recombination and is not appropriate here; the RBC-ET mechanism fails completely at high pressure in this system. This failure of the RBC-ET mechanism occurs because (see

Eq. (7) of paper I) it allows the QB state population to be kept depleted relative to its equilibrium value. Comparing the QB populations of Figures 2 and 3, one sees that, even at atmospheric pressures, the RBC-ET QB population shows significant depletion during most of the relaxation. At the higher H atom number densities in Table III, the RBC-ET QB number density is depleted by orders of magnitude. However, as shown by Figure 7, the exact QB number density rises rapidly and then stays near its equilibrium value. Indeed, except for the fact that the time scale is now femtoseconds instead of picoseconds, one can superpose Figure 7 on Figure 2 and only see a difference in the QB state populations at very short times. This behavior not only shows the limitations of the ET mechanism, but it also justifies fully the assumption, made and discussed in the construction of the master equations, that the BAB states always stay in equilibrium with the rest of the free continuum at high pressures. The assumption holds well for the QB states because of the large 3B rates connecting them to the continuum, and it will hold even better for the BAB resonances.

G. Collision Induced Dissociation

Calculations were also performed for the case of collision-induced dissociation (CID). In what is akin to a temperature-jump experiment in which a diatomic suddenly finds itself in a very high temperature environment, the initial number density of Ne_2 was taken to be 1.724×10^{12} cm^{-3}, all initially in the ground (0,0) state, the number density of H atoms was taken to be 2.4463×10^{20} (1 atm), the number density of Ne atoms is initially zero, and the temperature was again taken to be 30 K. The total number densities of the bound and QB states as a function of time from the exact solution of the master equations are shown in Figure 8. Using Eq. (20) to model the bound state population as a simple exponential decay gives an effective rate constant k_d for dissociation that starts small but rises to become almost constant. At 1000 psec it has the value of 3.911×10^{-11} cm^3/sec to be compared with the value 4.056×10^{-11} obtained for k_d in the recombination calculations at the same pressure. The reason these differ by about 3% is that neither has reached its equilibrium value; if

we instead begin with the populations of the bound and QB states in a 30 K equilibrium distribution, set the *Ne* number density to zero, and follow the relaxation in time, the effective k_d starts out *larger* than its final value and then, in a fashion qualitatively similar to Figure 5, decreases to become almost constant and has a value of 4.055×10^{-11} at 1000 psec. That the rate coefficients we obtain from these simple treatments of recombination and dissociation so nearly satisfy detailed balance is refreshing. It has been long known from master equations studies[9,12,13] that trying to extract simple "rate constants" at times when the populations of the internal rovibrational states are not in equilibrium relative to one another often gives results which significantly violate detailed balance. Such would happen here if rate coefficients were extracted at times too early in the relaxation.

The pressure dependence of the effective CID rate coefficients is similar to that discussed for recombination. Those obtained from fitting the exact solutions of the master equations vary only slightly with pressure. Those obtained from the RBC-ET approximation show falloff and vary from being a factor of 2.3 too small at the lowest pressures to a factor of a thousand too small at the highest pressures. They can be obtained from Table III and the equilibrium constant noted earlier.

H. Temperature Dependence

The recombination calculations of the previous subsections have been repeated for the range of temperatures justified by the range of energies of the calculations of paper I. The effective rate coefficients for *H* at low number density (2.4463×10^{17} molecules/cc) are in Table IV. One sees, as expected, that the dissociation rate increases as temperature increases, and that the recombination rate decreases as temperature increases. The results for the recombination rate coefficients are also plotted versus temperature in Figure 9, and the behavior is typical of recombination rate coefficients.

The VRIOS cross sections of paper I could easily be calculated to higher energies and rate constants and master equations generated at higher temperatures. In fact, because

the VRIOS approximation becomes more accurate at higher energies, the results would be more accurate than those presented here. We have not done so because the equilibrium number density of Ne_2 species is so low at high temperatures that it does not seem of much interest. We have not reported calculations to lower energies and temperatures because the VRIOS approximation becomes less accurate there. However, qualitatively, we expect the recombination rate to continue to increase as the temperature decreases below the lowest value shown on the plot. Although the QB (0,12) state will quit contributing when the temperature falls much below 12 K, the broad QB (1,6) state will continue contributing until T falls well below 2 K. Furthermore, the direct 3B recombination has paths with no barrier that contribute to all low temperatures.

III. DISCUSSION. SIMPLE KINETICS MODELS

A. Simple Kinetics Models

In this section we consider the question of to what extent simple models can describe the kinetics of CID and recombination of the present and other systems. It is again convenient to view the set of master equations of the previous section as an exact kinetic system and the results of the various accurate calculations with them as experimental results for the system. Clearly, the amount of detail required in a model will depend on the amount and accuracy of the experimental and theoretical data available. If one knew all the concentrations of all the states as functions of time and pressure (as in Fig. 1), one would need to have the full set of master equations of the previous section in order to fit all the data, and the resulting rate constants would indeed be constants independent of concentrations. However, one usually has much less information than that, and the model needs to be correspondingly simpler.

It is convenient to think in terms of a small set of species and reactions and to take a model that includes as many of them as are necessary to fit the available data while trying not to do anything unphysical. The following set of equations symbolizes the actual

processes known to be occurring:

$$A + B + M \rightleftharpoons AB^e + M, \tag{25}$$

$$A + B \rightleftharpoons AB^*, \tag{26}$$

$$A + B + M \rightleftharpoons AB^* + M. \tag{27}$$

$$AB^* + M \rightleftharpoons AB^e + M, \tag{28}$$

and

$$AB^e + M \rightleftharpoons AB^g + M. \tag{29}$$

Here AB^* represents the metastable states; if A and B are atoms, these are the QB states. AB^e represents the "excited" states of AB that get directly coupled to the metastable states and the continuum, and AB^g represents the "ground" or low-lying states of AB that are only connected to the other states by rovibrational relaxation. In these reactions Eq. (25) represents the direct 3B mechanism. Eqs. (26) and (28) represent the Lindemann[14] ET mechanism, and Eq. (29) symbolizes the Hinshelwood[15] additions to the Lindemann mechanism. Eq. (27), the 3B collisional mechanism for populating and equilibrating the metastable states, is new. It is essential to keep the metastable states from getting depleted at high pressures and is one of the most significant discoveries of the present work.

If one only knew the equilibrium dissociation constant for the bound molecules ($K_{eq} = 3.470 \times 10^{20}$ in the present system) and recombination data equivalent to the second column of Table III over too small a pressure range to see its variation with pressure, one would be justified in keeping only Eq. (25) of the above set of equations and dropping the superscript e distinction on the AB^e. That is equivalent to Eq. (20) and would give a $k_r^{(3)}$ of about 1.2×10^{-31} and a k_d of about 4.2×10^{-11} for the present system. When A and B are atoms, the simple Eq. (20) may often suffice to fit all available data.[16]

However, if one has accurate data over a wide enough third-body pressure range, as exemplified by all of the second column of Table III, the rate coefficients obtained via the preceding paragraph are not constant. Then, the simple 3B mechanism alone is not adequate, and one needs to add Eqs. (26) through (28) to the analysis. This makes a set of 4 equations involving 8 rate coefficients. However, the forward and reverse directions of each reaction are connected by equilibrium, and one can often make good estimates of the equilibrium constants needed. Also, Eqs. (26) and (27) have the same equilibrium constant, and the product of the equilibrium constants of Eqs. (26) and (28) is equal to the equilibrium constant for Eq. (25). That reduces the number of rate cofficients needed to four. Treating the kinetics of Eqs. (25) through (28) and assuming a steady-state approximation for the concentration $[AB^*]$ of metastables, one gets a relaxation equation of the form of Eq. (23) with $k_r^{(2)} = k_r^{(3)}[M]$ and $\kappa_d = k_r^{(2)} K_{eq}$ as before, except that now

$$k_r^{(3)} = k_{25} + \frac{(k_{26} + k_{27}[M])k_{28}}{\{k_{-26} + (k_{-27} + k_{28})[M]\}}. \tag{30}$$

Here the numbers on the rate coefficients refer to the model reactions and their reverses. We note in passing that this recombination rate cannot go over to bimolecular behavior at high third-body pressures unless both k_{25} and k_{27} are small.

Because k_{28} and k_{-28} are related by an equilibrium constant, there are four independent parameters in this equation. Unfortunately, the data in Table III can only uniquely determine three of them. However, one often can get information about the metastable states and their lifetimes and can then determine the remainder of the parameters. Using the present system as an example, we note that the equilibrium constants at 30 K for reactions (25) through (28), treating $AB^e = AB$ as containing all the bound states and AB^* as containing all the QB states, for the reactions in the direction written are $K_{25} = 2.882 \times 10^{-21}$, $K_{26} = K_{27} = 1.608 \times 10^{-21}$, and $K_{28} = 1.792$. Since the present simple model does not distinguish narrow from broad QB states, we sum the second row of Table II to get the total rate of tunneling into the QB states as $k_{26} = 4.40 \times 10^{-11}$. With the equilibrium constant just listed, that gives an effective outward tunneling rate of

$k_{-26} = 2.74 \times 10^{10}$. Then, a simple approximate fit of Eq. (30) to the data in the second column gives $k_{28} = 3.2 \times 10^{-11}$, $k_{-28} = 1.8 \times 10^{-11}$, $k_{27} = 2.6 \times 10^{-31}$, $k_{-27} = 1.6 \times 10^{-10}$, $k_{25} = 7.1 \times 10^{-32}$, and $k_{-25} = 2.5 \times 10^{-11}$. We note that these rate coefficients all have physically reasonable sizes, they are independent of concentrations, they give the pressure dependence of the overall reaction rate, and they give a reasonable balance of three-body and sequential two-body contributions. However, they still have limitations: The value of k_{25} thus obtained is a factor of two smaller than its true value of 1.504×10^{-31} obtained from summing the first eight lines of the last column of Table III.

To get a more realistic model one must include Eq. (29). That requires, in addition to the information used for the simpler models, the rovibrational relaxation rate of the molecule. It allows one to get (as seen in Figure 5a) a steady-state recombination rate which is slower than the initial pure 3B recombination rate. And the resulting rate coefficients more closely approach their true values. However, analytic solutions do not give formulas simple enough to be very enlightening, so we do not give details here. We simply note that inclusion of Eq. (29) will often be helpful.

We also note that if one has enough information, one will want to extend the set of model equations to include more than one excited bound state. Also, if A and B are atoms, it is usually easy to calculate the energies, angular momenta, and lifetimes of the QB resonant states. Their lifetimes usually vary by many orders of magnitude, and one may want to use more than one AB^* state to represent them.

The most important point of this discussion of simple models is that, for systems in which A and B are atoms and diatomics molecules, one should not use a model which includes Reaction (26) without also including Reactions (25) and (27). Otherwise, one is likely to obtain rate coefficients that either have unphysical sizes or give give unphysical results at some third-body pressures.

B. Other Simple Systems

We have seen in this work that 3B processes dominate and that the ET mechanism is a minor contributor to our example reaction. Now let us consider applications to other atomic recombination and diatomic CID reactions. For the recombination of most atoms A and B the rates of the various processes symbolized by Eqs. (25) through (29) will, of course, be different than for our example system. However, all those processes will still occur, and there is every reason to expect true 3B collisions to be every bit as important in the formation of excited bound states and QB states. In fact, those QB states which lie near enough the top of their angular momentum barrier that their tunneling rates are significant are precisely those which lie close enough to the continuum to be rapidly formed by 3B collisions. Thus, as we reviewed in paper I, all available experimental and theoretical evidence indicates that 3B processes dominate atomic recombination reactions in general. Their most obvious difference from our example system is that in recombination most of their population will relax into the AB^g states.

In particular, consider the recombination of H atoms in noble gases, a standard prototype reaction. Although H_2 has many more total bound and QB states than Ne_2, H_2 has only 6 QB states that are low enough in energy and broad enough to contribute significantly to the RBC-ET mechanism,[2] compared to 2 broad QB states of Ne_2. Hence, the systems are more alike than one might at first think. Thus, as reviewed in paper I and despite earlier claims[2] to the contrary, ortho-para ratios, the pressure dependence, careful classical calculations, and several master equation studies give very strong evidence that 3B processes dominate over the RBC-ET mechanism in H atom recombination.

In connection with the present and following discussion, we note that if electronically excited states of the atoms or molecules or nonadiabatic processes can contribute[17], the behavior can be more complicated and should be treated appropriately. In the case of recombination of ions, we also note that species such as AM^+ usually have bound states, and one must then consider including the BC mechanism. Also, it should be noted that all

$A^+ - B^-$ systems have an infinite number of bound levels whose wavefunctions extend to very large r which are connected to the continuum by 3B collisions.

C. Polyatomic Systems

If AB is a polyatomic molecule, all the processes symbolized by Eqs. (25) through (29) still occur. However, their relative rates can be very different from the diatomic case. Polyatomic molecules have very many more vibrational and rotational states than do diatomic molecules. This allows many pathways for the relaxation of Eq. (29) that have small energy gaps and proceed much more rapidly. Furthermore, these levels extend above the dissociation limit to produce very large numbers of vibration-rotation metastable states AB^* which have enough energy to dissociate but for which the energy is in non-dissociative vibrational modes. Such AB^* states are easily and rapidly formed *classically* via Eq. (26); they require no tunneling for formation. Their vibrational redistribution times are long enough, and the dissociative motions are a small enough fraction of the available phase space that they easily live long enough to contribute. These differences tend to make the Lindemann-Hinshelwood[14,15] ET mechanism relatively more important than in the case in which AB is a diatomic.

When A is an atom and B is a diatom,[18,19] and even when both A and B are diatoms,[20] the experimental second-order recombination rate coefficient, which is proportional to the concentration of the inert third body gas at low pressures, is often observed to show curvature but to never become flat (second order) until such high pressures that diffusion limiting and cage effects are dominating rather than recombination. In such cases the behavior of equations such as Eq. (30) imply that Reaction (26) is very important but that Reactions (25) and (27) are also significant and cannot be neglected. The interplay of all the possible processes can make the observed pressure dependence really quite complicated.[21]

When both A and B are polyatomics or when either A or B is a large polyatomic (four or more atoms), for the systems of which we are aware,[18,22] the observed second-

order recombination rate coefficient is proportional to the third-body concentration at low pressures but curves over and is flat (second order) over a rather wide pressure range at higher pressures. Such behavior implies[24] via Eq. (30) that Reaction (26) is so dominant that Reactions (25) and (27 are then negligible. Then, (for inert third bodies M) the Lindemann-Hinshelwood[14,15] mechanism suffices, and the usual RRKM methods[23] are applicable.

IV. CONCLUSIONS

In this paper we have generated and solved the master equations governing the kinetics of the recombination and collision-induced dissociation (CID) reaction $Ne+Ne+H \rightleftharpoons Ne_2+H$. The effects of pressure and temperature were explored. It was found that three-body (3B) collisions dominated over sequential two-body collisions at all pressures. The sequential two-body (energy-transfer) mechanism gives a rate that is more than a factor of two too small at very low pressures and orders of magnitude too small at high third-body pressures. It was found that rates directly connecting both the excited bound states and the quasibound (QB) states to the nonresonant 3B continuum are essential to the kinetics.

The relevance of the present simple reaction to other recombination and CID reactions was discussed. All evidence available indicates that 3B collisions are dominant if the fragments are atoms. Available evidence also indicates that if neither fragment is more complicated than a diatomic, then three-body and sequential two-body (ET) mechanisms are competitive and neither is usually dominant. When the fragments are themselves polyatomics, the sequential two-body (ET) mechanism is usually dominant.

V. ACKNOWLEDGEMENT

This work was performed under the auspices of the US Department of Energy under the Laboratory Directed Research and Development Program.

REFERENCES

[1] R. T Pack, R. B. Walker, and B. K. Kendrick, J. Chem. Phys. **00**, 0000 (1998), preceding paper, and references therein.

[2] R. E. Roberts, R. B. Bernstein, and C. F. Curtiss, Chem. Phys. Letters **2**, 366 (1968) and J. Chem. Phys. **50**, 5163 (1969); R. E. Roberts and R. B. Bernstein, Chem. Phys. Letters **6**, 282 (1970); P. A. Whitlock, J. T. Muckerman, and R. E. Roberts, J. Chem. Phys. **60**, 3658 (1974).

[3] M. A. Eliason and J. O. Hirschfelder, J. Chem. Phys. **30**, 1426 (1959).

[4] See, for example, R. D. Levine, *Quantum Mechanics of Molecular Rate Processes* (Oxford U. Press, London, 1969), pp. 85 and 147.

[5] See, for example, R. K. Preston and R. T Pack, J. Chem. Phys. **69**, 2823 (1978).

[6] See, for example, T. L. Hill, *An Introduction to Statistical Thermodynamics* (Addison-Wesley, Reading, MA, 1960), Chapters 8 and 10.

[7] See M. R. Flannery, J. Chem. Phys. **95**, 8205 (1991) and references therein.

[8] J. T. Lowry and R. F. Snider, J. Chem. Phys. **61**, 2320 (1974); R. T. Snider and J. T. Lowry, *ibid.* **61**, 2330 (1974).

[9] H. O. Pritchard, Specialist Periodical Reports, Reaction Kinetics (Chem. Soc., London) **1**, 243 (1975).

[10] J. E. Dove and S. Raynor, J. Phys. Chem. **83**, 127 (1979).

[11] D. W. Schwenke, J. Chem. Phys. **92**, 7267 (1990).

[12] J.E. Dove and D. G. Jones, Chem. Phys. Letters **17**, 134 (1972).

[13] T. Ashton, D. L. S. McElwain, and H. O. Pritchard, Can. J. Chem. **51**, 237 (1973).

[14] F. A. Lindemann, Trans. Faraday Soc. **17**, 598 (1922).

[15] C. N. Hinshelwood, Proc. Roy. Soc. **A113**, 230 (1927).

[16] D. L. Baulch, et al., J. Phys. Chem. Ref. Data **21**, 411 (1992).

[17] See for example, R. J. Browne and E. A. Ogryzlo, J. Chem. Phys. **52**, 5774 (1970) and J. E. Smedley, H. K. Haugen, and S. R. Leone, *ibid.* **86**, 6801 (1987).

[18] See, for example, J. Troe, *Physical Chem.: An Advanced Treatise* **6B**, 835 (1975).

[19] See, for example, C. J. Cobos, H. Hippler, and J. Troe, J. Phys. Chem. **89**, 342 (1985).

[20] R. Forster, M. Frost, D. Fulle, H. F. Hamann, H. Hippler, A. Schlepegrell and J. Troe, J. Chem. Phys. **103**, 2949 (1995).

[21] S. Baer, H. Hippler, R. Rahn, M. Siefke, N. Seitzinger and J. Troe, J. Chem. Phys. **95**, 6463 (1991); H. Hippler, R. Rahn, and J. Troe, *ibid.* **93**, 6560 (1990).

[22] See, for example, H. Hippler, K. Luther, A. R. Ravishankara, and J. Troe, Z. Phys. Chem. Neue Folge **142**, 1 (1984).

[23] R. G. Gilbert and S. C. Smith, *Theory of Unimolecular and Recombination Reactions* (Blackwell, Oxford, 1990); T. Baer and W. L. Hase, *Unimolecular Reaction Dynamics: Theory and Experiments* (Oxford U. Press, New York, 1996).

[24] C. E. Klots, J. Chem. Phys. **53**, 1616 (1970).

TABLES

TABLE I. Rate Coefficients at $T = 30$ K from states i=(v,j) into states f=(v',j'). The continuum is listed as (C). The first 11 columns have units of 10^{-11} cc/molecule-sec; the last column has units of 10^{-32} cc^2/molecule^2-sec.

f←i	(0,0)	(0,2)	(0,4)	(0,6)	(0,8)	(1,0)	(1,2)	(1,4)	(1,6)	(0,10)	(0,12)	(C)
(0,0)	.00	3.74	1.09	.30	.07	.16	.05	.01	.00	.02	.00	.05
(0,2)	17.82	.00	7.43	2.25	.62	.28	.27	.10	.02	.15	.03	.29
(0,4)	8.35	11.93	.00	7.81	2.50	.18	.22	.25	.06	.70	.16	.68
(0,6)	2.74	4.38	9.45	.00	8.01	.18	.18	.20	.15	2.62	.67	1.47
(0,8)	.70	1.24	3.12	8.26	.00	.18	.19	.20	.14	8.05	2.42	3.07
(1,0)	.08	.03	.01	.01	.01	.00	3.13	.99	.27	.08	.07	.48
(1,2)	.13	.14	.07	.05	.05	15.18	.00	6.47	1.69	.05	.05	2.72
(1,4)	.05	.08	.14	.09	.09	8.10	10.88	.00	5.60	.11	.15	6.28
(1,6)	.01	.02	.05	.09	.08	2.87	3.75	7.39	.00	.13	.26	12.77
(0,10)	.15	.28	.81	2.50	7.45	.14	.18	.24	.21	.00	7.44	6.05
(0,12)	.02	.05	.16	.55	1.93	.10	.15	.27	.35	6.41	.00	11.23
(C)	.70	.82	1.21	2.18	4.39	12.84	14.92	20.44	31.50	9.36	20.19	.00

TABLE II. Rate Coefficients at $T = 30$ K for tunneling out of and into each of the quasibound states of Ne_2. The third line is the number density of third-body atoms at which the 3B collisional and tunneling rates of formation of the QB state i are equal.

$i =$	(1,6)	(0,10)	(0,12)
$k_{tout}(\text{sec}^{-1})$	5.12×10^{10}	7.69×10^{5}	4.18×10^{10}
k_{tin}(cc/molecule-sec)	2.07×10^{-11}	4.97×10^{-16}	2.33×10^{-11}
$n_H^{equal}(i)$ molecules/cc	1.63×10^{20}	8.22×10^{15}	2.07×10^{20}

TABLE III. Effective Third Order Rate Coefficients $k_r^{(3)}$(cc^2/ molecule^2-sec) at $T = 30$ K for the Recombination of Ne atoms in H as a function of H atom number density in molecules/cc.

n_H	Exact	RBC-ET
2.4463×10^{17}	1.221×10^{-31}	5.261×10^{-32}
2.4463×10^{18}	1.217×10^{-31}	5.164×10^{-32}
2.4463×10^{19}	1.207×10^{-31}	4.956×10^{-32}
2.4463×10^{20}	1.169×10^{-31}	3.537×10^{-32}
2.4463×10^{21}	1.141×10^{-31}	9.090×10^{-33}
2.4463×10^{22}	1.137×10^{-31}	1.065×10^{-33}
2.4463×10^{23}	1.136×10^{-31}	1.085×10^{-34}

TABLE IV. Effective Rate Coefficients at low number density as a function of temperature for Ne in H. k_d (10^{-11}cc/molecule-sec) is the second order dissociation rate coefficient, and $k_r^{(3)}(10^{-31}\text{cc}^2/\text{molecule}^2\text{-sec})$ is the third order recombination rate coefficient.

T(Kelvin)	k_d	$k_r^{(3)}$
20	2.580	1.675
25	3.387	1.390
30	4.237	1.221
35	5.118	1.107
40	6.030	1.025
45	6.962	0.961

FIGURES

FIG. 1. Number densities (molecules/cm^3) of the states of Ne_2 versus time in recombination. The bound states are symbols connected by solid lines; the QB states are symbols connected by dashed line. The symbols and the states they represent, with i being the master equation index and (v,j) the spectroscopic index, are: solid circles, i=1=(0,0); asterisks, i=2=(0,2); solid squares, i=3=(0,4); solid triangles, i=4=(0,6); X, i=5=(0,8); open triangles, i=6=(1,0); Y, i=7=(1,2); diamonds, i=8=(1,4); stars, i=9=(1,6); crossed boxes, i=10=(0,10); and tvtables, i=11=(0,12).

FIG. 2. Total number densities of the bound states (solid circles) and QB states (stars) as functions of time in picoseconds for the same recombination simulation as in Figure 1. Accurate solution of full set of master equations. See text for discussion.

FIG. 3. Prediction of the RBC-ET sequential two-body collision mechanism for the total number densities of the bound states (solid circles) and QB states (stars) as functions of time in picoseconds for the same conditions as in Figure 2.

FIG. 4. Prediction of a "3B only" calculation which allows 3B collisions but does not allow quantum tunneling. Total number densities of the bound states (solid circles) and QB states (stars) as functions of time in picoseconds for the same conditions as in Figure 2.

FIG. 5. Effective third order recombination rate coefficient as a function of time. The solid circles are for the exact solution of the master equations; the stars are for the RBC-ET approximation. Same conditions as Figs. 1-3.

FIG. 6. Effective recombination rate coefficients versus third body number density. The points are for the exact solution of the master equations; the stars are for the RBC-ET approximation. (a) semilog plot of third-order coefficients. (b) log-log plot of second-order coefficients. See text for discussion.

FIG. 7. High pressure behavior. Total number densities of bound and QB states of Ne_2 versus time in femtoseconds. The number density of H atoms here is 2.4463×10^{23} molecules/cc. Exact solution.

FIG. 8. Collision-induced dissociation. Total number densities of bound and QB states of Ne_2 versus time in picoseconds at 1 atmosphere third-body pressure. Exact solution.

FIG. 9. Temperature dependence of effective third order recombination rate coefficients. Exact solution.

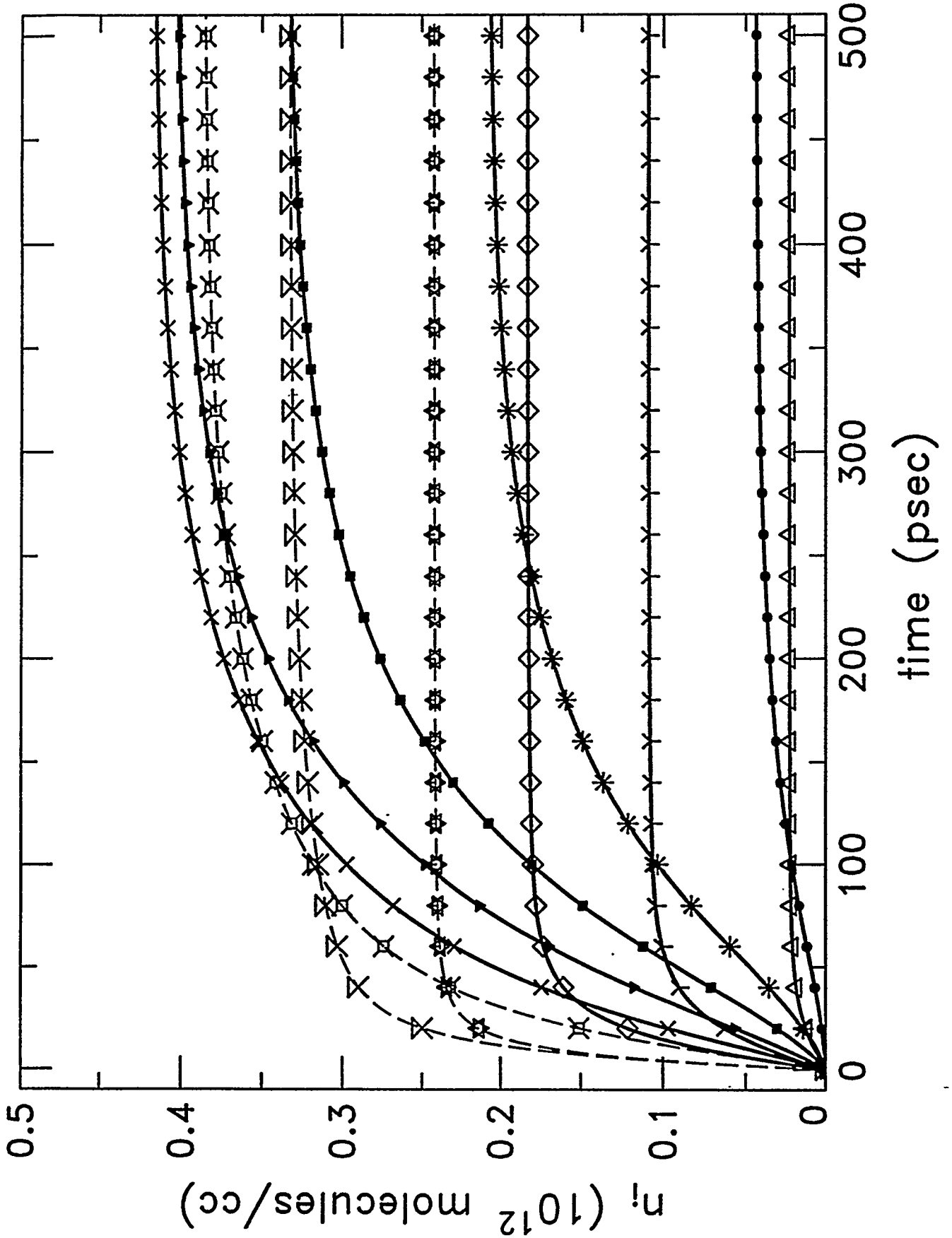
0.5
0.4
0.3
0.2
0.1
0
0
100
200
300
400
500
time (psec)
n_i (10^{12} molecules/cc)

Figure 1

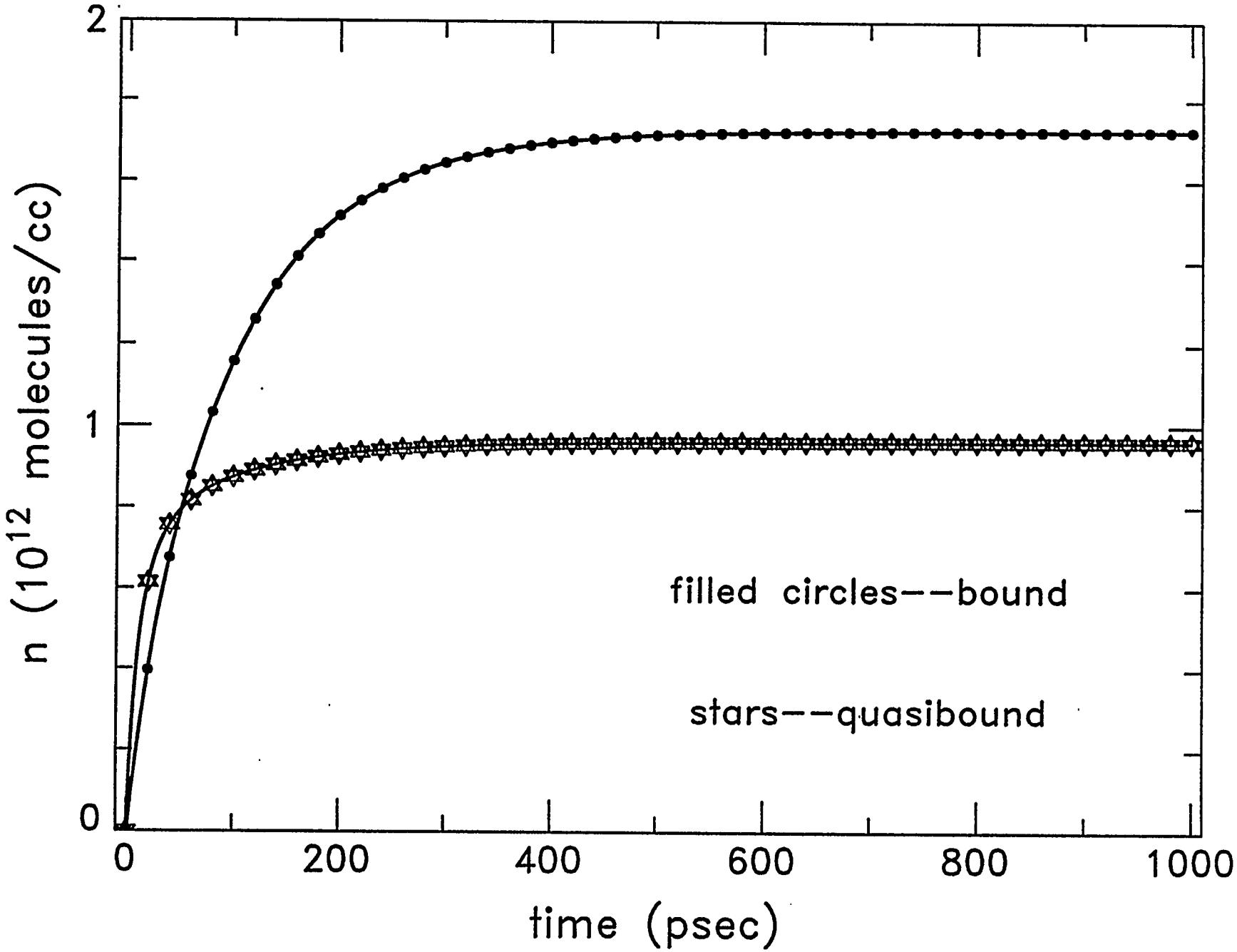
2
1
0
n (10^{12} molecules/cc)
0
200
400
600
800
1000
time (psec)
filled circles--bound
stars--quasibound

Figure 2

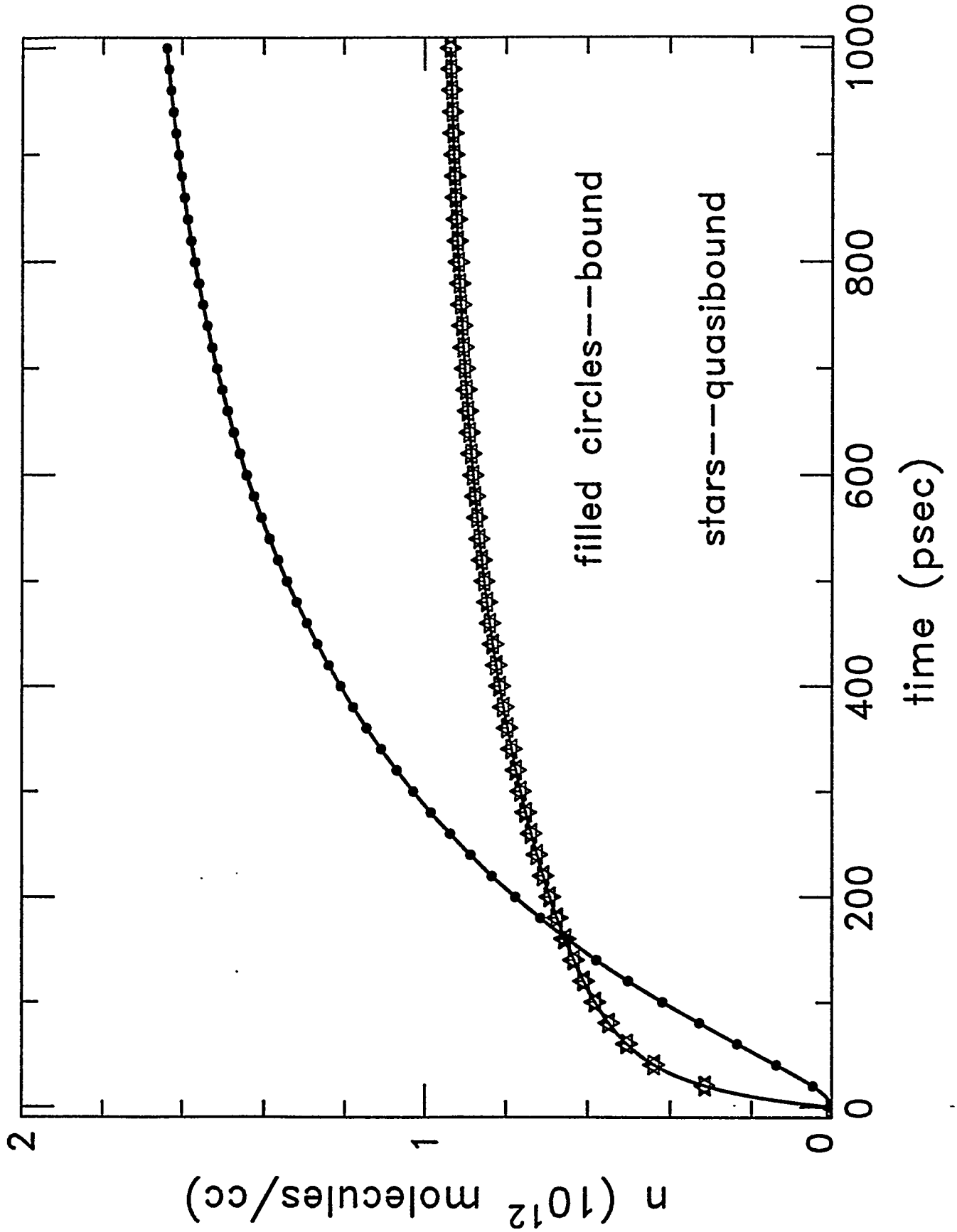
n (10^{12} molecules/cc)
2
1
0
0
200
400
600
800
1000
time (psec)
filled circles--bound
stars--quasibound

Figure 3

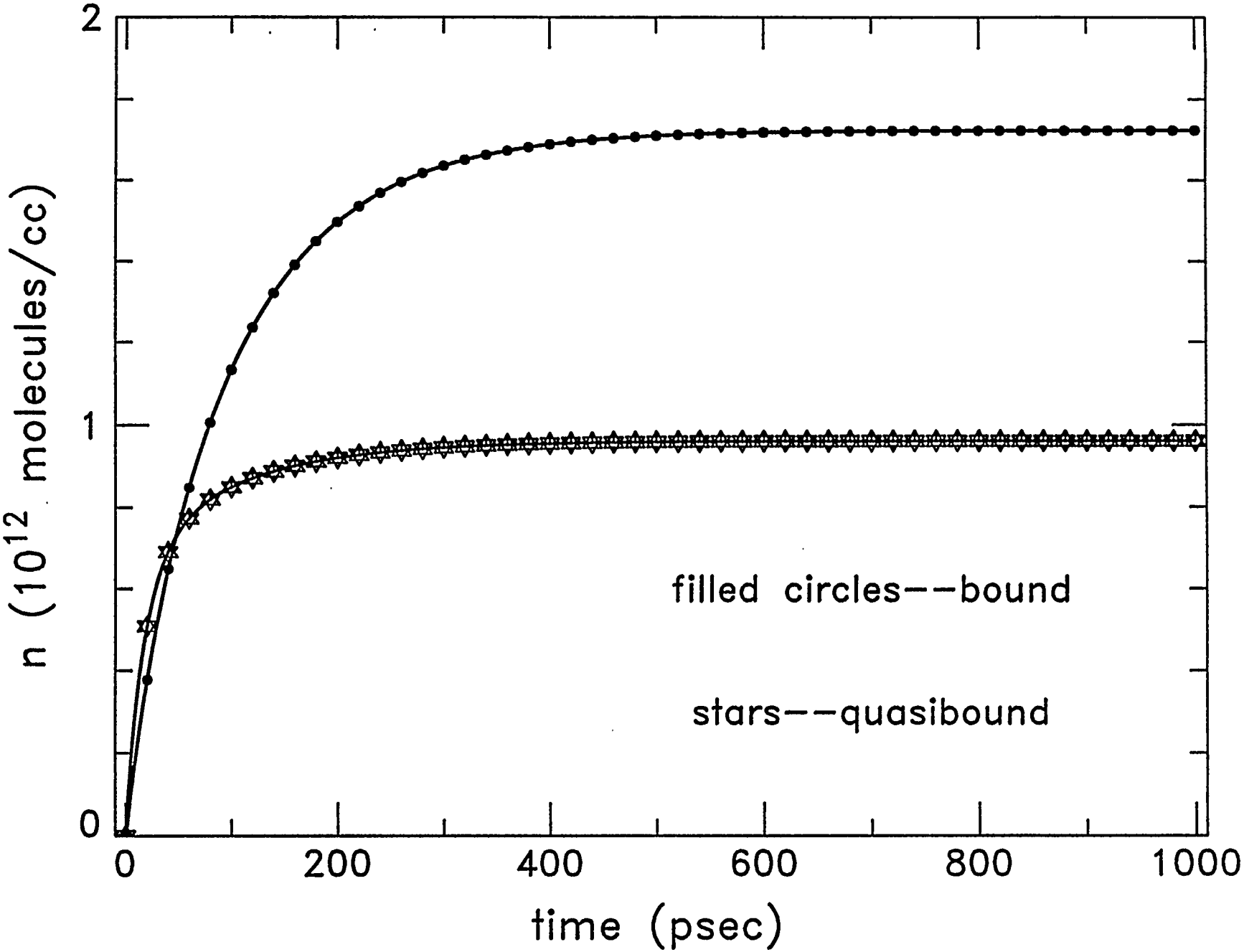
2
1
0
n (10^12 molecules/cc)
0
200
400
600
800
1000
time (psec)
filled circles--bound
stars--quasibound

Figure 4

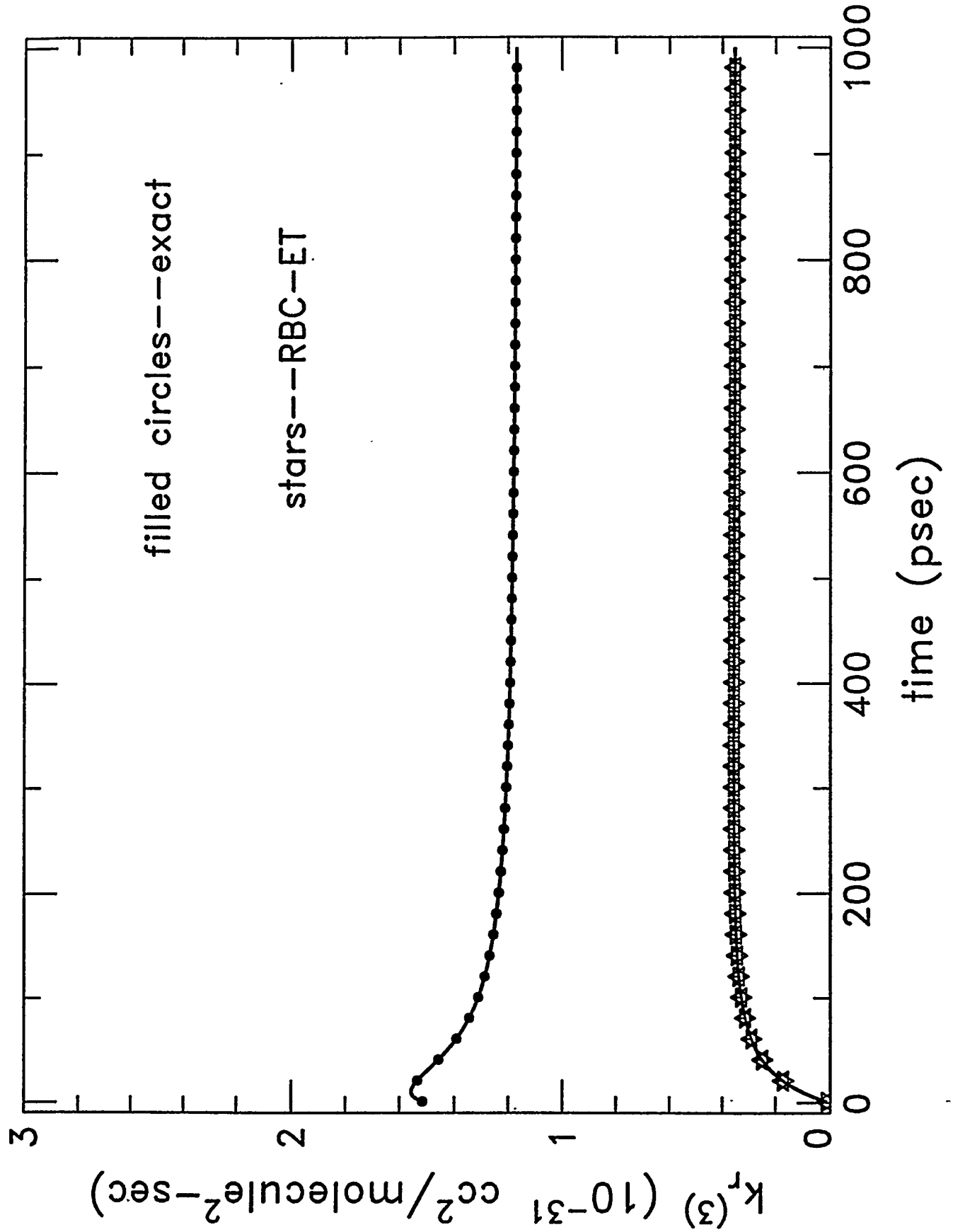
filled circles--exact
stars--RBC-ET
$k_r^{(3)}$ (10^{-31} cc^2/molecule^2-sec)
time (psec)
0
1
2
3
0
200
400
600
800
1000

Figure 5

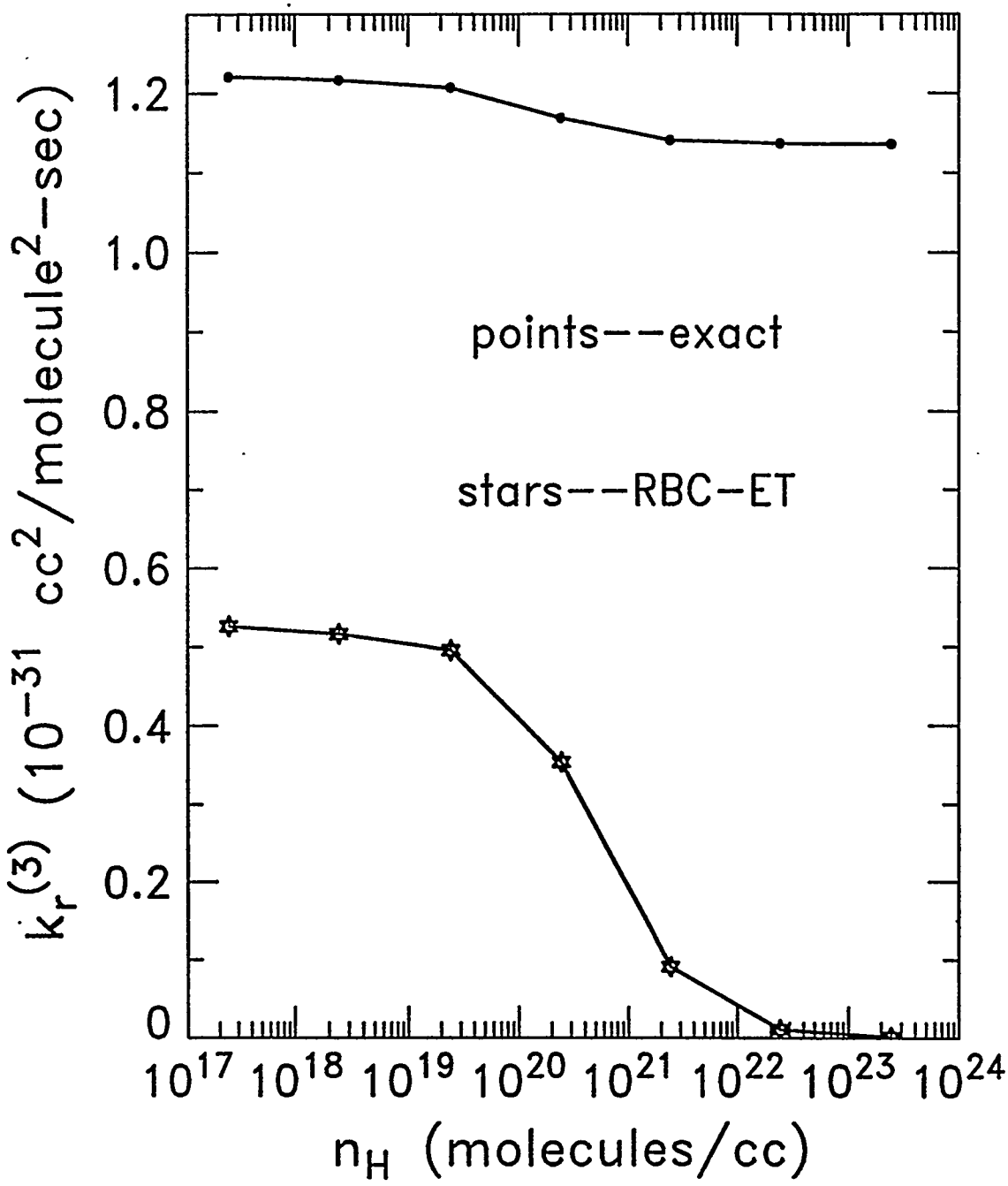
1.2
1.0
0.8
0.6
0.4
0.2
0
points--exact
stars--RBC-ET
$k_r^{(3)}$ (10^{-31} cc^2/molecule^2-sec)
10^{17} 10^{18} 10^{19} 10^{20} 10^{21} 10^{22} 10^{23} 10^{24}
n_H (molecules/cc)

Figure 6 (a)

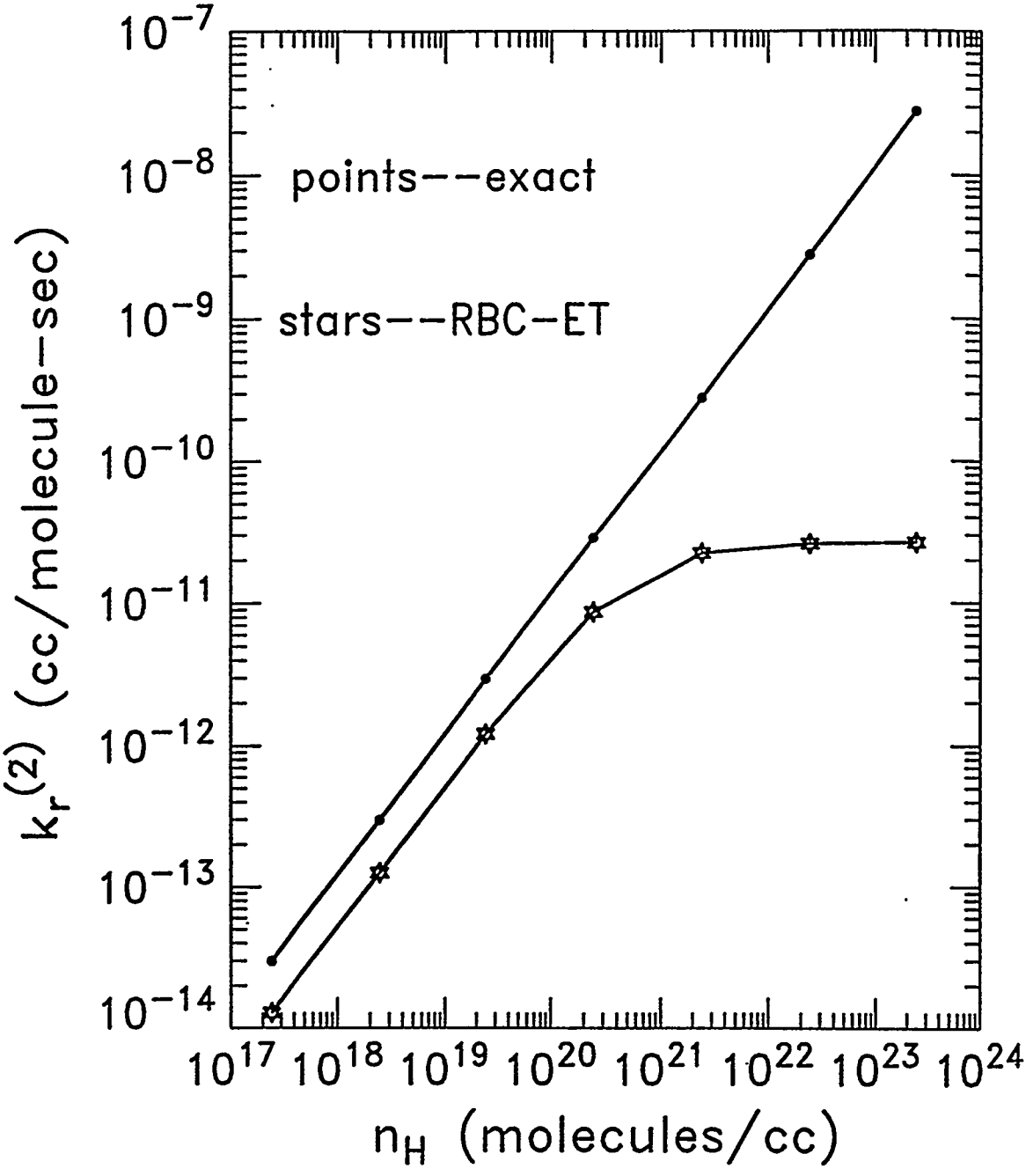
10^{-7}
10^{-8}
10^{-9}
10^{-10}
10^{-11}
10^{-12}
10^{-13}
10^{-14}
points--exact
stars--RBC-ET
$k_r^{(2)}$ (cc/molecule-sec)
10^{17} 10^{18} 10^{19} 10^{20} 10^{21} 10^{22} 10^{23} 10^{24}
n_H (molecules/cc)

Figure 6(b)

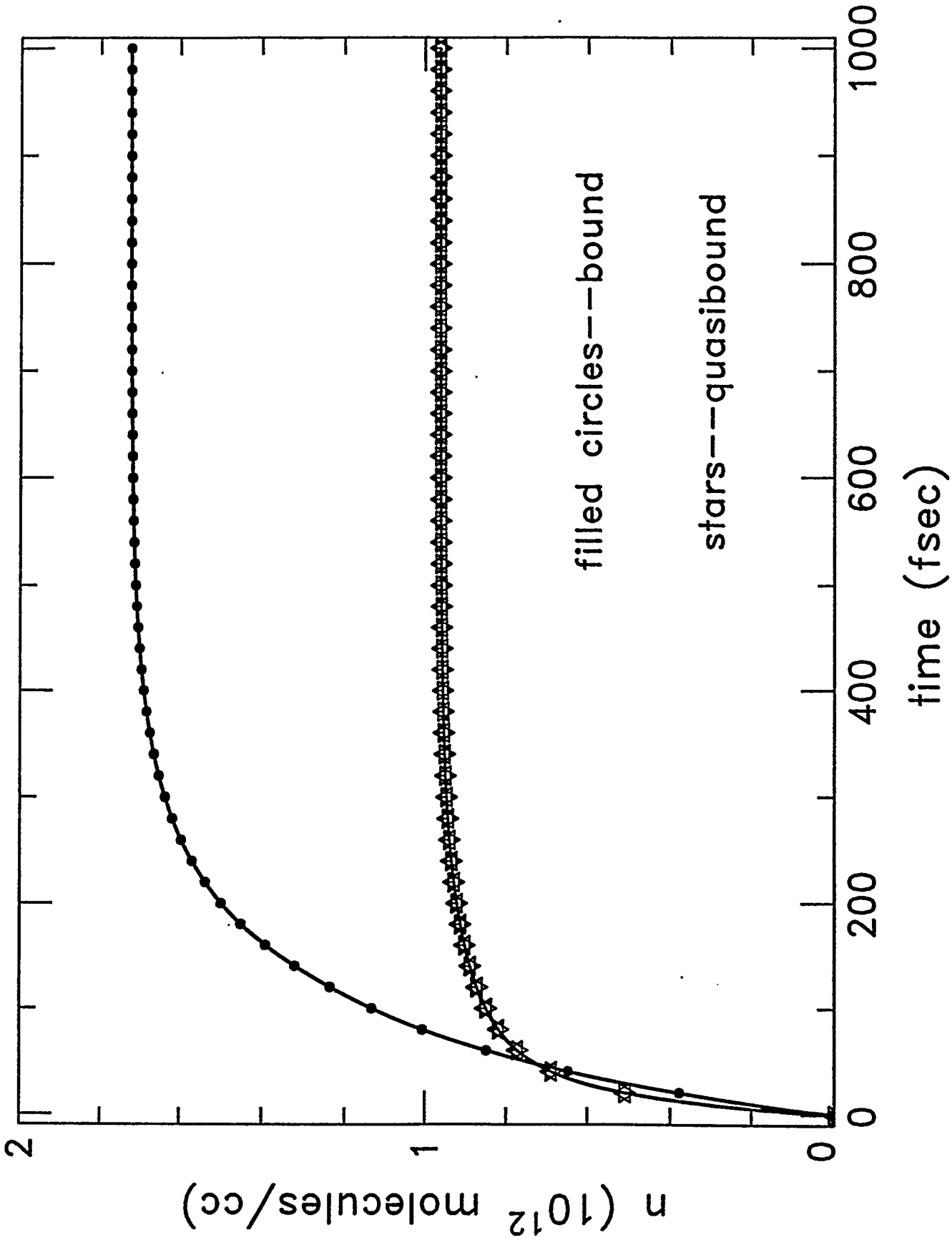
filled circles--bound
stars--quasibound
time (fsec)
n (10^{12} molecules/cc)
0
200
400
600
800
1000
1
2

Figure 7

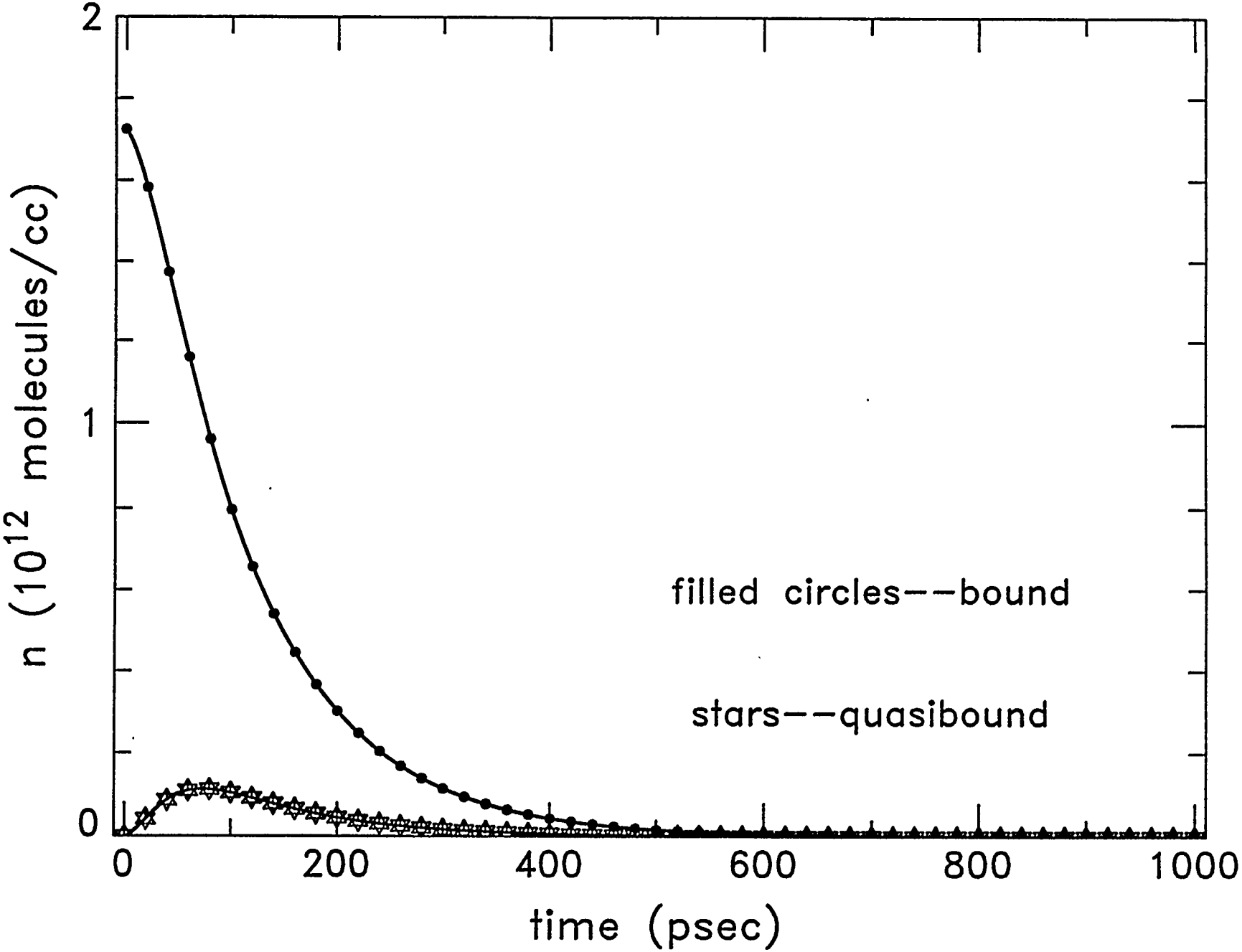
2
1
0
n (10^12 molecules/cc)
filled circles--bound
stars--quasibound
0
200
400
600
800
1000
time (psec)

Figure 8

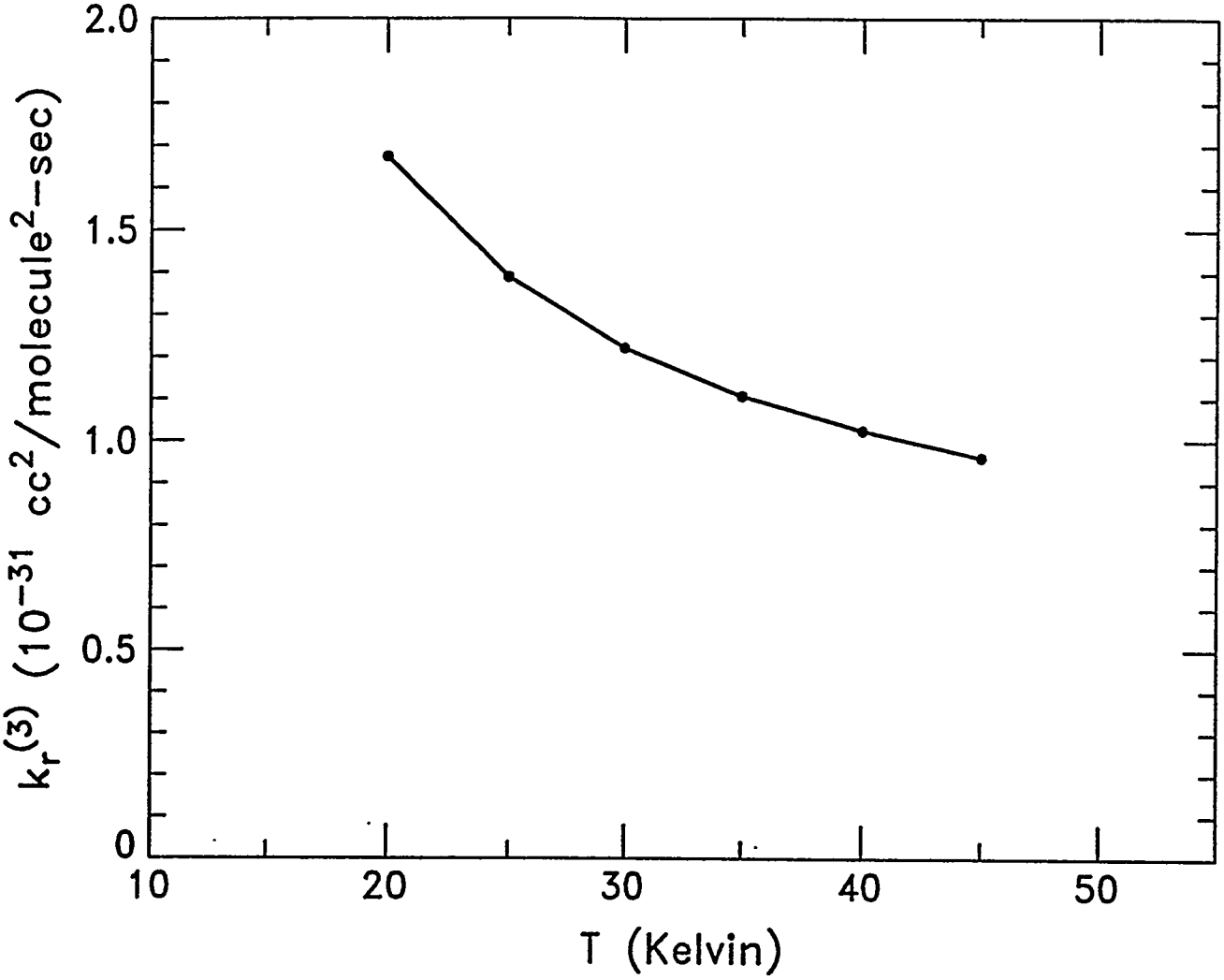

Figure 9